Non-collinear quasi phase matching and annular profiles in difference frequency generation with focused Gaussian beams

P. Malara[*1,3], **P. Maddaloni**[1], **G. Mincuzzi**[1], **S. De Nicola**[2] **and P. De Natale**[1]

[1] *Consiglio Nazionale delle Ricerche – Istituto Nazionale di Ottica Applicata and European Laboratory for Nonlinear Spectroscopy (LENS),Comprensorio "A. Olivetti," Via Campi Flegrei 34, 80078 Pozzuoli (Naples), Italy*

[2] *Consiglio Nazionale delle Ricerche - Istituto di Cibernetica "E. Caianello," Comprensorio "A. Olivetti," Via Campi Flegrei 34, 80078 Pozzuoli (Naples), Italy*

[3] *Dipartimento di Scienze Ambientali, Seconda Università di Napoli, Via Vivaldi 43, I-81100 Caserta, Italy*

**Corresponding author: pietro.malara@inoa.it*

Abstract: We present and experimentally test a simple model for difference frequency generation (DFG) in periodically-poled crystals with gaussian pumping beams. Focusing of input beams originates several non-collinear quasi-phase-matching configurations of the interacting wavevectors, which contribute to the idler output field. In this picture, we accurately describe a number of effects, such as the occurrence of annular idler intensity profiles and the asymmetric trend of DFG power vs temperature. Finally, we quantitatively test the model by means of an indirect measurement of the crystal poling period.

OCIS codes: (190.4223) Nonlinear wave mixing, (190.4420) Transverse effects in nonlinear optics

References and Links

1. H. Huang and K.K. Lehmann, "Noise in cavity ring-down spectroscopy caused by transverse mode coupling," Opt. Express **15**, 8745-8759 (2007)
2. J. L. Hall and C. Bordé, "Measurement of methane hyperfine structure using laser saturated absorption" Phys. Rev. Lett. **30**, 1101-1104 (1973)
3. R. G. Hunsperger, *Integrated Optics - Theory and technology*, (Springer 2002)
4. S. Kulin, S. Aubin S. Christe, B. Peker, S. L. Rolston and L. A. Orozco, " A single Hollow-beam optical trap for cold atoms," J. Opt. B: Quantum semiclass. Opt. **3**, 353-357 (2001)
5. A. Kaplan, N. Friedman and N. Davidson "Optimized single beam dark optical trap," J. Opt. Soc. Am. B, **19**, 1233-1238 (2002)
6. G. Giusfredi, D. Mazzotti, P. Cancio and P. De Natale, "Spatial mode control in radiation generated by frequency difference in periodically poled crystals," Phys Rev. Lett. **87**, 113901 (2001)
7. D. Richter, P. Weibring, A. Fried, "High-power, tunable difference frequency generation source for absorption spectroscopy based on a ridge waveguide periodically poled lithium niobate crystal," Opt. Express **15**, 564-571 (2007)
8. G. Imeshev, M. Proctor, and M. M. Fejer, "Lateral patterning of nonlinear frequency conversion with transversely varying quasi-phase-matching gratings," Opt. Lett. **23**, 673-675 (1998)
9. G.D. Boyd, D.A. Kleinman, "parametric interaction of focused Gaussian light beams," J. Appl. Phys. **39**, 3597-3641 (1968)
10. Jean-Jacques Zondy, "The effects of focusing in type-I and type-II difference-frequency generations," Opt. Commun. **149**, 181-206 (1998)
11. S. K. Wong, G. Fournier, P. Mathieu and P. Pace. "Beam divergence effects on nonlinear frequency mixing," J. Appl. Phys. **71**, 1091-1101 (1992)
12. D. Lu, L. Qian, Y. Li, H. Yang, H. Zhu and D. Fan, "Phase velocity nonuniformity-resulted beam patterns in difference frequency generation," Opt. Express **15**, 5050-5056 (2007)
13. J. R. Morris, Y.R. Shen, "Theory of far-infrared generation by optical mixing," Phys. Rev. A **15**, 1143-1156 (1977)

#91370 - $15.00 USD Received 7 Jan 2008; revised 21 Mar 2008; accepted 30 Mar 2008; published 20 May 2008

14. Husam H. Abu-Safe, "Difference frequency mixing of strongly focused Gaussian beams in periodically poled $LiNbO_3$," Appl. Phys. Lett. **86,** 231105 (2005)
15. G. M. Gibson, G. A. Turnbull, M. Ebrahimzadeh, M. H. Dunn, H. Karlsson, G. Arvidsson and F. Laurell, "Temperature-tuned difference-frequency mixing in periodically poled $KTiOPO_4$" Appl. Phys. B: Lasers. Opt **67**, 675-677 (1998)
16. K. Fradkin, A. Arie, A. Skliar, and G. Rosenman, "Tunable midinfrared source by difference frequency generation in bulk periodically poled KTiOPO4," Appl. Phys. Lett. **74**, 914-917 (1999)
17. F. Zernike, J. E. Midwinter, *Applied Nonlinear Optics*, (J. Wiley & Sons, 1973)
18. P. Maddaloni, G.Gagliardi, P. Malara and P. De Natale, "A 3.5-mW continuous-wave difference-frequency source around 3 mm for sub-Doppler molecular spectroscopy," Appl. Phys. B **80**, 141-145 (2005)
19. D. H. Jundt, "Temperature dependent Sellmeier equation for the index of refraction, n_e, in congruent lithium niobate," Opt. Lett. **22**, 1553-1555 (1997)

1. Introduction

A thorough control of the spatial mode of coherent radiation beams is essential for several basic applications, such as coupling to optical resonators (or any long-path setup) [1], sub-Doppler spectroscopic techniques [2], waveguided optics [3] and optical trapping [4,5]. Nonlinear sources and difference frequency generators (DFGs) in particular, have proven to be an important tool for implementing the mentioned techniques in the mid-infrared. However, several observations reported in literature point out that DFGs exhibit a diversified range of idler intensity profiles, from bell-like to ring-like, or a combination of the two [6,7]. This aspect may strongly affect their performance. In periodically poled (PP) nonlinear crystals, the use of transversely varying quasi-phase-matching (QPM) gratings has been proposed to engineer the requested idler profile [8]. Anyway, although nonlinear frequency mixing has been extensively investigated from a conversion efficiency point of view [9-11], to our knowledge, only few works have dealt with the effects on the emission mode of DFG radiation [6,12,13]. Moreover, in most of these cases, the approach was strictly numerical.

In the present work we report a combined theoretical and experimental study of the intensity profile of DFG radiation produced in a periodically-poled lithium niobate (PPLN) crystal with focused gaussian input beams. Several effects already reported in literature, such as the existence of annular beam patterns at certain temperatures, the non-gaussian profile of the maximum-intensity idler beam [6] as well as the asymmetry observed in the $sinc^2$ law [14-16], are explained through an analysis of the non-collinear quasi phase matching configurations that arise when two focused beams interact in a PPLN crystal. In the case of interaction between a plane wave and a focused Gaussian beam, an analytical treatment is given, leading to a generalization of the ordinary plane collinear wave DFG theory. In spite of the simplificative assumptions, this analytical model is able to accurately reproduce the behaviour of DFG radiation also when both focused input beams are used, demonstrating the possibility of a full control of the idler beam spatial mode. Finally, the model performance is quantitatively tested through an indirect measurement of the crystal poling period.

2. Theory

In this section we consider a DFG process between two focused Gaussian beams propagating through a birefringent periodically poled (PP) crystal, collinearly to the poling grating wave vector $\mathbf{k_g}$. As a first step, only the interaction in a plane orthogonal to the crystal axis (plane x=0 in Fig.1) is taken into account. This assumption allows to treat the crystal as isotropic, and will be reconsidered later on.

The interacting beams field amplitude in the focal plane is $E(y)=E_0 \exp(-y^2/w^2)$, where w is the waist and y the distance from the centre of the spot at $z=0$. This field can be decomposed in a set of plane waves of wave vector $\mathbf{k}$, according to the Fourier representation $E(\mathbf{y}) = \int E(\mathbf{k}) e^{i\mathbf{k}\cdot\mathbf{y}} d\mathbf{k}$.

#91370 - $15.00 USD Received 7 Jan 2008; revised 21 Mar 2008; accepted 30 Mar 2008; published 20 May 2008

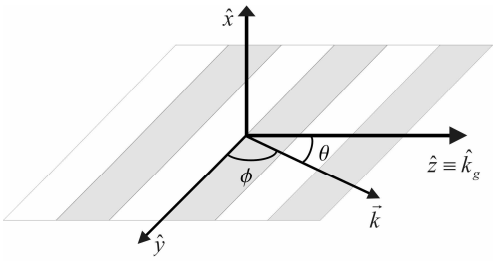

Fig. 1. Frame adopted to describe the nonlinear interaction in a plane orthogonal to the crystal axis

If ϑ is the angle between the wave vector **k** and the grating wave vector $\mathbf{k_g}$, which we take in the z direction (see Fig. 1), the spatial Fourier representation of a beam propagating along $\mathbf{k_g}$ can be arranged, for small ϑ, as

$$E(\vartheta) = E_0 \frac{w^2}{4\pi} e^{-\frac{w^2 k^2 \vartheta^2}{4}} \tag{1}$$

Eq. (1) is the angular amplitude distribution of the plane wave components in which a gaussian beam can be decomposed and will be used in the following. At large distances from the focal plane, the beam is represented by a spherical wave with centre of curvature in *z=0* and gaussian angular amplitude distribution centered at $\vartheta=0$.

In the ordinary DFG theory the nonlinear conversion is governed by the mismatch vector $\mathbf{\Delta k}=\mathbf{k_s}-\mathbf{k_p}-\mathbf{k_i}-\mathbf{k_g}$, where the indexes *s, p, i, g* refer respectively to *signal*, *pump*, *idler* and *grating* wave vector). In the case of plane waves propagating along $\mathbf{k_g}$, all the wave vectors are parallel and the mismatch is a scalar quantity [17]:

$$\Delta k_0(T, \lambda_s, \lambda_p) = 2\pi \left(\frac{n(T, \lambda_s)}{\lambda_s} - \frac{n(T, \lambda_p)}{\lambda_p} - \frac{n(T, \lambda_i)}{\lambda_i} - \frac{1}{\Lambda(T)} \right). \tag{2}$$

Once the DFG parameters (pumping wavelengths λ_s and λ_p, the nonlinear crystal refractive index $n(\lambda,T)$ and the poling period Λ) are fixed, Δk_0 only depends on temperature *T*. This dependence is linear in a large interval around the quasi-phase-matching temperature T_0, and the idler intensity is given by the well known $sinc^2(\Delta k_0 L/2)$ law [17]. In the following, this case will be referred to as collinear quasi-phase-matching (CQPM).

For gaussian signal and pump beams, the angular spectrum decomposition given by Eq. (1) allows to analyze the nonlinear interaction in terms of coupling between their plane wave components, i.e. occurring between each signal plane-wave component $\mathbf{k_s}$ and all the pump plane-wave components $\mathbf{k_p}$. In the interaction plane considered (y-z), the resulting phase mismatch for a generic interacting couple ($\mathbf{k_s}$, $\mathbf{k_p}$) has components

$$\begin{cases} k_s \cos\vartheta_s - k_p \cos\vartheta_p - k_i \cos\vartheta - k_g = \Delta k_z \\ k_s \sin\vartheta_s - k_p \sin\vartheta_p - k_i \sin\vartheta = \Delta k_y \end{cases} \tag{3}$$

The angles ϑ_s (between $\mathbf{k_g}$ and $\mathbf{k_s}$), ϑ_p (between $\mathbf{k_g}$ and $\mathbf{k_p}$) and the idler radiating angle ϑ (between $\mathbf{k_g}$ and $\mathbf{k_i}$) are ultimately limited by the aperture arctg(*d/L)*, where *d* and *L* are respectively the thickness and the length of the poling channel. Assuming for these quantities typical values (one mm thickness and a few cm length), the above angles result very small.

#91370 - $15.00 USD Received 7 Jan 2008; revised 21 Mar 2008; accepted 30 Mar 2008; published 20 May 2008

Putting Δk_z and Δk_y =0, manipulating to eliminate ϑ and substituting goniometric functions with their second-order series expansion, we obtain a more general QPM condition, that includes the case of interaction between non-collinear waves:

$$k_s(k_p + k_g)\vartheta_s^2 + k_p(k_s - k_g)\vartheta_p^2 - 2k_s k_p \vartheta_s \vartheta_p + \Delta k_0(2k_i + \Delta k_0) = 0 \qquad (4)$$

Equation (4) identifies all the signal-pump couples $(\vartheta_s, \vartheta_p)$ whose interaction is quasiphasematched at a given temperature. Substituting a solution of (4) into (3), the corresponding idler emission angle ϑ is retrieved.

For Δk_0 <0, the solutions of Eq. (4) can be represented as points of a family of ellipses in the (ϑ_s-ϑ_p) plane, parametric in *T* (see Fig. 2). Each of these points is a non-collinear quasi phase-matching (NCQPM) configuration of vectors $\mathbf{k_s}$, $\mathbf{k_p}$, $\mathbf{k_g}$ and $\mathbf{k_i}$ and can be seen as one of the possible quadrangles that can be built with four vectors of moduli $k_s(T)$, $k_p(T)$, $k_i(T)$, $k_g(T)$ and the orientation of $\mathbf{k_g}$ fixed along *z*. As $\Delta k_0 \to 0$, the ellipse (4) degenerates in the (0,0) point, and the only allowed quadrangle is the one with the four vectors aligned, that corresponds to the common CQPM condition. For Δk_0 >0 no real solution of Eq. (4) exists.

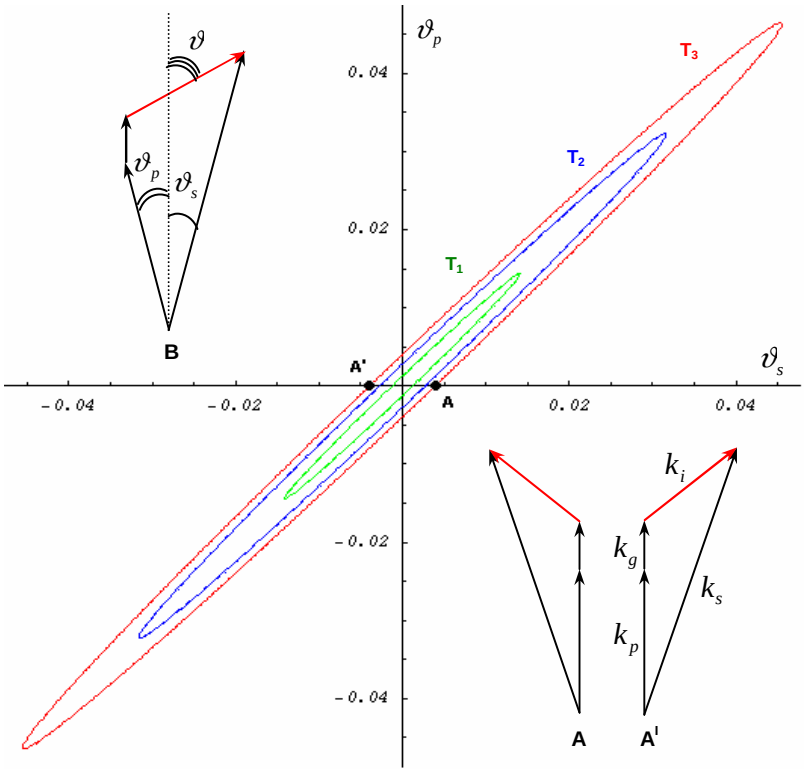

Fig. 2. Map, parametric in T, of plane wave interactions (ϑ_s, ϑ_p) that cancel the vector mismatch of Eq. (3). Schemes B, A and A' are examples of NCQPM configurations. In particular A and A' $(\pm\vartheta_s, 0)$ represent the configurations allowed in the case of interaction between a focused signal beam and a plane pump wave propagating along $\mathbf{k_g}$.

#91370 - $15.00 USD Received 7 Jan 2008; revised 21 Mar 2008; accepted 30 Mar 2008; published 20 May 2008

The idler field amplitude generated by a NCQPM couple $(\vartheta_s, \vartheta_p)$ along its radiating direction ϑ is proportional to the product of signal and pump amplitudes. From Eq. (1):

$$E_{idl}(\vartheta_s, \vartheta_p) \propto E_{0,s} E_{0,p} e^{-\frac{w_s^2 k_s^2 \vartheta_s^2 + w_p^2 k_p^2 \vartheta_p^2}{4}}. \tag{5}$$

The elements to reconstruct the idler field generated by all the couples that simultaneously satisfy NCQPM condition are now available. However, for the current investigation it is sufficient to spot the solution corresponding to the maximum idler field amplitude, and find its radiating direction. The derivation is particularly simple if $w_s k_s << w_p k_p$ that corresponds to a situation where signal beam is much more tightly focused than pump. In this case Eq. (5) reduces to $E_{0,s}^2 E_{0,p}^2 \exp(-w_p^2 k_p^2 \vartheta_p^2/4)$, therefore we expect the maximum of the idler intensity for the direction ϑ given by the *$(\vartheta_s, 0)$* solution (see schemes A and A' in fig. 2). In the limit of a collimated pump beam *$(\vartheta_s, 0)$* is the only NCQPM configuration allowed.

To retrieve the angle of maximum idler intensity ϑ we then substitute the solution *$(\vartheta_s, 0)$*, in the system (3). Within the small angle approximation, it writes

$$\begin{cases} k_s\left(1-\vartheta_s^2/2\right) - k_p - k_i\left(1-\vartheta^2/2\right) - k_g = 0 \\ k_s \vartheta_s - k_i \vartheta = 0 \end{cases}. \tag{6}$$

and, solved with respect to ϑ, gives

$$|\vartheta| = \sqrt{\frac{-2\Delta k_0}{k_i\left(1-k_i/k_s\right)}}. \tag{7}$$

Equation (7) represents a relation between the plane-collinear-wave mismatch $\Delta k_0(T)$ and the peak idler amplitude direction ϑ. Therefore it allows to define a generalized scalar mismatch

$$\Delta k_{eff}(T, \vartheta) = \Delta k_0 + \frac{k_i}{2}\left(1-\frac{k_i}{k_s}\right)\vartheta^2 \tag{8}$$

such that $\Delta k_{eff}(T, \vartheta)$ vanishes when a NCQPM condition is satisfied along direction ϑ.

The ordinary coupled equations for interaction between collinear plane waves [17] yield for the idler beam amplitude the expression:

$$E_i(T) \propto E_{0,s} E_{0,p} \int_{-L/2}^{L/2} e^{i\Delta k_0 z} dz \tag{9}$$

As mentioned before, within the approximation $w_s k_s << w_p k_p$, only configurations of type *$(\vartheta_s, 0)$* occurr. In this case Eq. (9) can be generalized to account for NCQPM by simply replacing the factor $E_s E_p$ with Eq. (5), and Δk_0 with the generalized Δk_{eff} of Eq. (9):

$$E_i(T, \vartheta) \propto E_{0,s} E_{0,p} e^{-\left(\frac{w_s k_i \vartheta}{2}\right)^2} \int_{-\frac{L}{2-\vartheta^2}}^{\frac{L}{2-\vartheta^2}} e^{i\Delta k_{eff} z} dz, \tag{10}$$

#91370 - $15.00 USD Received 7 Jan 2008; revised 21 Mar 2008; accepted 30 Mar 2008; published 20 May 2008

Where the condition $k_s \vartheta_s - k_i \vartheta = 0$ from Eq. (6) has been inserted to eliminate the ϑ_s dependence. Also, the integration limits take in account that the idler sums up coherently over a length that depends on ϑ. Finally, the square modulus of Eq. (10) yields the generalized *sinc*^{2} law:

$$I(T,\vartheta) \propto E_{0,s}^2 E_{0,p}^2 e^{-\frac{(w_s k_i \vartheta)^2}{4}} Sinc^2[\Delta k_{eff} \cdot \frac{L}{2-\vartheta^2}] \qquad (11)$$

which rules the emission intensity of the quasiphasematched DFG process. It is worth noting that for $\vartheta=0$, it gives back the conventional $sinc^2(\Delta k_0 L/2)$. The main peculiarity of this intensity law is that its maximum ($\Delta k_{eff}=0$) occurs for angles that depend on Δk_0. For this reason $\Delta k_0 = 0$ is a transition point, as far as the output intensity is concerned. In fact, since the term $k_i(1-k_i/k_s)\vartheta^2$ in Eq. (8) is always positive, a NCQPM configuration (and thus an angular idler emission), can occur only for $\Delta k_0 < 0$. For $\Delta k_0 = 0$ CQPM is allowed, with axial intensity emission, while for a positive Δk_0 no real solution of Eq. (8) exists, and an ordinary $sinc^2(\Delta k_0 L/2)$ tail in axial direction is expected for the intensity.

Substituting in Eq. (2) the Sellmeier equations [18] for the behaviour of refractive indexes, it is easy to see that Δk_0 mismatch scales linearly with T over a range of several degrees around its zero-point T_0, (see inset of Fig. 3). Therefore, the axial-to-angular idler transition described above is expected when T crosses T_0. This is shown in Fig. 3, where $I(T,\vartheta)$ is plotted around T_0 in the paraxial direction (DFG parameters: λ_s =1053.05 nm, λ_p = 1551.60 nm and Λ_0 =29.89 μm).

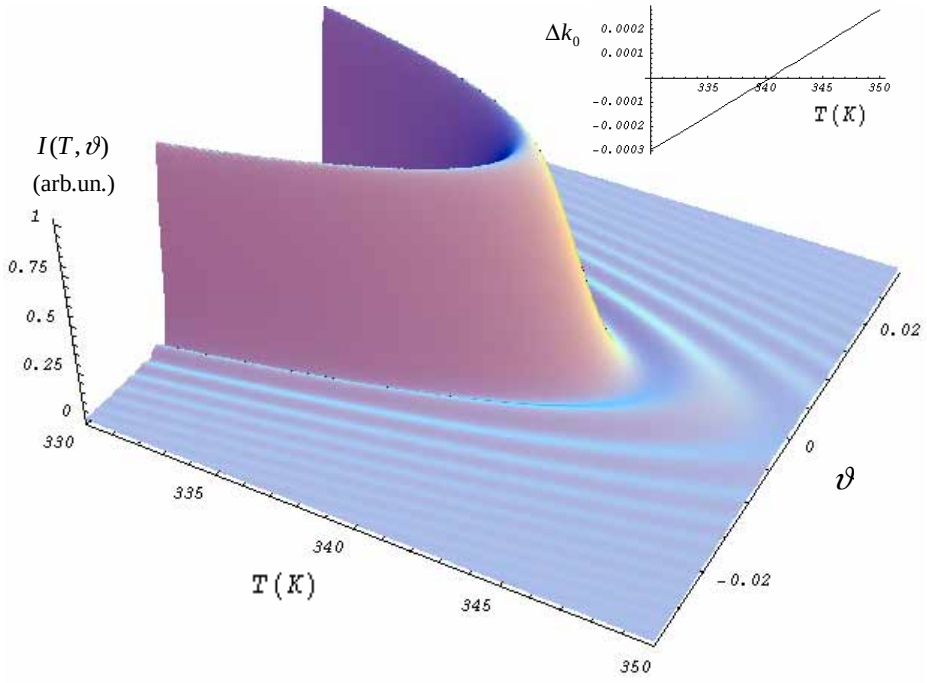

Fig. 3. Normalized idler intensity $I(T, \vartheta)$ in paraxial direction, in proximity of the collinear quasi phase matching temperature T_0=*340.4 K* Calculated for λ_s =1053.05 nm, λ_p =1551.60 nm and Λ_0= 29.89 μm. Below T_0, due to NCQPM, the idler intensity is peaked around angles that depart from the axial direction as the temperature decrease.

#91370 - $15.00 USD Received 7 Jan 2008; revised 21 Mar 2008; accepted 30 Mar 2008; published 20 May 2008

As a side note, since Δk_0 also depends on λ_s and λ_p, analogous transitions are expected when tuning pump or signal wavelength across their CQPM value. However, since the gradients of Δk_0 with respect to T and λ_p are opposite in sign, crossing the CQPM point by tuning in the same direction either pump wavelength or temperature is expected to result in reversed spatial-mode evolutions.

All the described approach can be applied to the orthogonal plane ($y=0$, where $\mathbf{k_g}$ and the crystal optical axis lay) as well. For small angles, the angular dependence of the refractive indexes due to the birefringence has no appreciable effect. Indeed, in a real 3D crystal, according to Eq. (11), the idler beam should exhibit a spot-like far-field pattern for $\Delta k_0 > 0$, that reaches its maximum intensity at $\Delta k_0 = 0$. Then, for $\Delta k_0 < 0$, the beam energy should move to cones of aperture 2ϑ, thus resulting in an annular far-field pattern with increasing diameter as Δk_0 decreases.

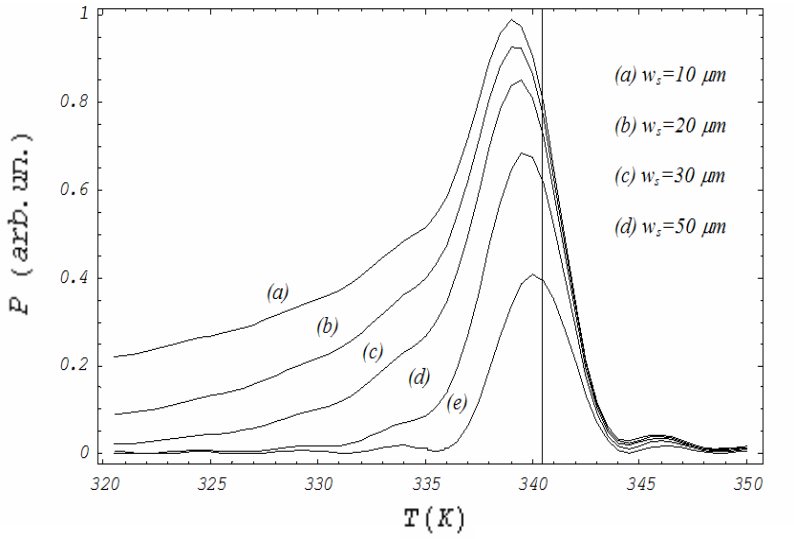

Fig. 4. Numerical evaluation of Eq. (12): overall output power for a difference frequency generation with focused signal beam (λ_s=1053.05 nm, λ_p =1551.60 nm and Λ_0=29.89 μm). Different curves correspond to different values of the signal waist w_s. The vertical line indicates the collinear QPM temperature T_0 .

The overall emitted idler power for each crystal temperature can be found simply integrating the intensity distribution given by Eq. (11) over all the angular spread within the poling channel aperture:

$$P(T) \propto E_{0,s}^2 E_{0,p}^2 \int_{-\frac{d}{L}}^{\frac{d}{L}} e^{-\frac{(w_s k_i \vartheta)^2}{4}} Sinc^2\left(\Delta k_{eff} \cdot \frac{L}{2-\vartheta^2}\right) d\vartheta . \qquad (12)$$

A numerical evaluation of such quantity is plotted in Fig. 4 for different values of the signal waist w_s. It is worth noting that, while for CQPM the condition of maximum output power is $\Delta k_0 = 0$, in presence of a focused signal beam the maximum always occurs for temperatures below T_0 ($\Delta k_0 < 0$). This means that the far-field beam pattern corresponding to the maximum

#91370 - $15.00 USD Received 7 Jan 2008; revised 21 Mar 2008; accepted 30 Mar 2008; published 20 May 2008

emitted idler power is annular, as already observed by Giusfredi et al [6]. As shown in Fig. 4, such effect becomes more evident as the focusing increase.

Another interesting feature of Fig. 4 is the asymmetric behaviour exhibited by *P(T)* around T_0, which also becomes more evident for tightly-focused signal beam. This effect, already treated in several works [14,15], is in this framework directly related to the energy transfer into annular patterns occurring for $T<T_0$. In this connection, it is worth noting that experimental $P(\lambda_p)$ curves reported in literature [16] exhibit a reversed asymmetry with respect to the *P(T)* curves of Fig. 4. This is consistent with our previous statement, that tuning either T or λ_p across their CQPM value is expected to result in reversed spatial profile evolutions.

3. Experimental setup and results

In our DFG setup (described into details in a previous work [18]) the signal beam comes from an extended cavity diode laser (ECDL) (Toptica, DL100) tuned at λ_s=1053.05 nm, and amplified to a power of 100 mW by an Yb-amplifier. The pump radiation, coming from a second ECDL (New Focus, Velocity), is tuned at λ_p =1551.60 nm and boosted up to 8 W by an Er-doped fiber amplifier. The two laser beams, properly polarized and collimated, are combined onto a dichroic mirror and focused by a near-IR achromatic lens (f=100 mm) in the center of the nonlinear crystal; the signal and pump diameters in the waist are respectively 30 and 50 μm. The nonlinear element is an antireflection-coated, PP $LiNbO_3$ crystal (Deltronic), consisting of an array of 9 different channels each of length L=50 mm, width and thickness d=1 mm, with poling periods ranging from 29.6 to 30.6 μm. The crystal temperature is stabilized by means of a Peltier cell driven by a PID temperature-controller. The idler radiation (≈1 mW), filtered from the unconverted near-IR light by an AR-coated germanium window, propagates freely for 120 mm before impinging onto the detector's sensing surface. The latter is a mid-infrared, cryogenically-cooled camera (Indigo, MerlinLab), consisting of an array of 320x256 Indium Antimonide detectors, each with diameter of 30 μm.

To test the occurrence of the behaviour described in the preceding paragraph, the far-field DFG beam intensity profiles were acquired for different crystal temperatures. Data are shown in Fig. 5 (each frame has its own normalized grey scale), together with the theoretical prediction by Eq. (11). Above the CQPM temperature, the idler beam maintains a well bell-shaped profile whose intensity increases with decreasing T, until its maximum value is reached at T_0 (frame #2). Below this temperature, we start to observe a dip in the center of the beam whose depth increases as the temperature departs from T_0, eventually leading to an hollow profile (frames 3 to 7). The weak spots and concentric rings due to the secondary maxima of the generalized $sinc^2$ are also visible (frames 1,2,5,6).

For each temperature, the overall emitted power was also measured. The asymmetry predicted for this quantity can be appreciated in Fig. 6, where *P(T)* is plotted together with the theoretical prediction by Eq. (12) for w_s=15 μm. The occurrence of the reversed transition by pump wavelength tuning was also verified.

#91370 - $15.00 USD Received 7 Jan 2008; revised 21 Mar 2008; accepted 30 Mar 2008; published 20 May 2008

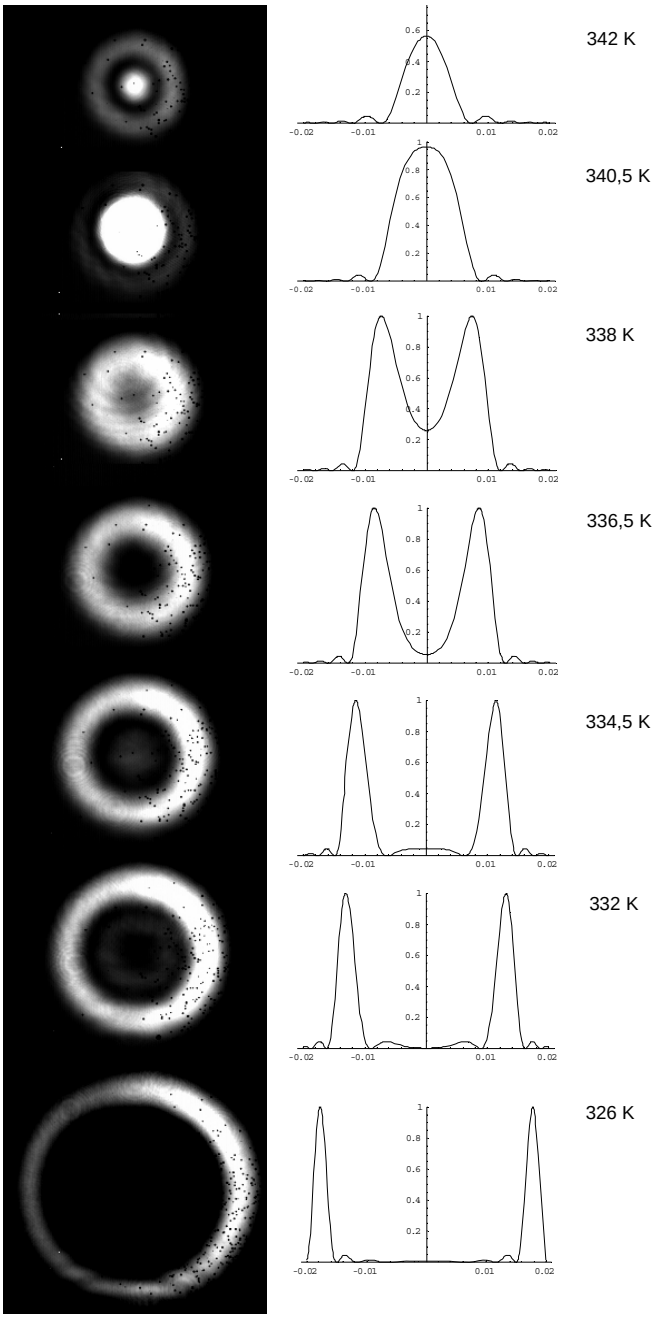

Fig. 5. Recorded intensity distributions of the far field DFG beam for increasing values of temperature. On the right side, the corresponding theoretical *I(T, ϑ)* predicted by Eq. (11) are also reported.

#91370 - $15.00 USD Received 7 Jan 2008; revised 21 Mar 2008; accepted 30 Mar 2008; published 20 May 2008

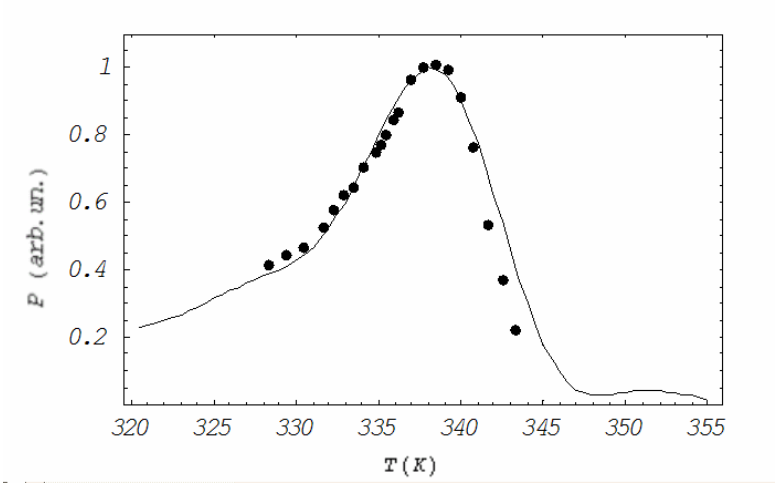

Fig. 6. Asymmetry in the output DFG power vs temperature, attributed to NCQPM at $T<T_0$ in presence of focused beams (w_s=20 μm, w_p=50 μm). Continuous line: theoretical prediction by Eq. (12) for a focused-signal beam DFG (w_s=15 μm) and a plane pump wave.

For a more quantitative test of the model, a measurement of the crystal poling period was performed according to the following procedure. Any temperature below T_0 allows a NCQPM configuration, resulting in an annular intensity pattern with horizontal half aperture ϑ. Such angle was measured for different temperatures and the resulting set of points (T, ϑ) fitted with Eq. (7). In the fitting procedure, the effect of the refractive index discontinuity at the crystal boundary and a possible offset in the temperature probe calibration t_0 were considered. The thermal expansion of the crystal was also taken in account, by using a poling period $\Lambda = \Lambda_0\left[1+\alpha(T-298)+\beta(T-298)^2\right]$. Numerical values for α and β as well as the Sellmeier equations implicit in the fitting function are reported in [19].

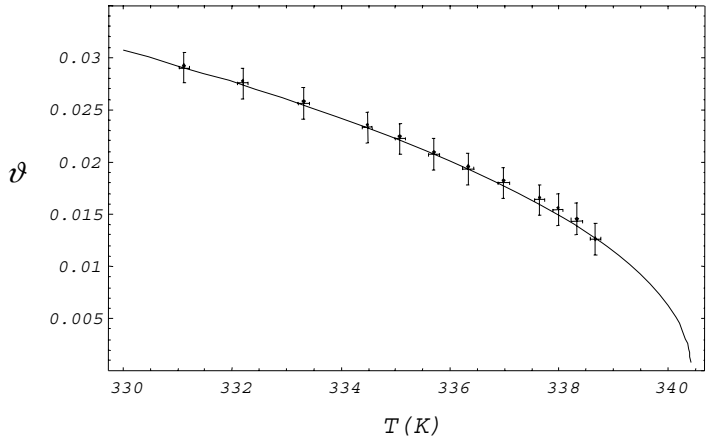

Fig. 7. Half aperture angle of NCQPM idler emission for $T<T_0$. The continuous line is the fitting curve given by Eq. (7), used to extract the poling period at room temperature.

#91370 - $15.00 USD Received 7 Jan 2008; revised 21 Mar 2008; accepted 30 Mar 2008; published 20 May 2008

The resulting poling period is Λ_0 = 29.89(1) μm (to be compared with the nominal 29.9 μm given by the crystal manufacturer) and t_0 = 0.72 K. The agreement of data with the model can be appreciated in Fig. 7. The half-aperture angle, as expected, drops down to zero at the CQPM temperature T_0 =340.45 K.

4. Conclusions

Focusing of input beams in difference frequency generation allows several non-collinear quasi-phase-matched configurations to radiate. As a result, many effects take place, such as annular idler beam intensity profiles and asymmetry in the sinc^2 intensity law. An extension of the ordinary plane-wave DFG theory that includes non-collinear quasi-phase-matching provides a physically meaningful, analytical description for the above mentioned intensity distribution effects. Though derived exactly in the case of interaction between a focused signal and a collimated pump beam, this model is able to reproduce the behaviour of a DFG process with both focused input beams as well. In the latter case, a direct comparison with experimental observations was also performed, demonstrating that such generalized DFG relations reproduce accurately all the observed features of the idler radiation intensity profiles. Such analytical description has been also used for a quantitative measurement of the crystal poling period, resulting consistent with the value given by the manufacturer.

Acknowledgements

The authors are grateful to G. Gagliardi, G. Giusfredi, M. De Rosa and P. Ferraro for helpful discussions and accurate reading of the manuscript. This work was partially funded by Ente Cassa di Risparmio di Firenze.

#91370 - $15.00 USD Received 7 Jan 2008; revised 21 Mar 2008; accepted 30 Mar 2008; published 20 May 2008